Available online at www.sciencedirect.com
SCIENCE DIRECT®
Journal of Catalysis 227 (2004) 352–366
JOURNAL OF CATALYSIS
www.elsevier.com/locate/jcat

Co-beta zeolite highly active in propane–SCR-NO_x in the presence of water vapor: effect of zeolite preparation and Al distribution in the framework

Libor Čapek, Jiří Dědeček, Blanka Wichterlová *

J. Heyrovský Institute of Physical Chemistry, Academy of Sciences of the Czech Republic, CZ-182 23 Prague 8, Czech Republic

Received 21 April 2004; revised 22 July 2004; accepted 3 August 2004

Available online 3 September 2004

Abstract

$CoNH_4$-beta and CoH-beta zeolites, with various Co loadings, were prepared by Co ion exchange into NH_4- and H-beta parent zeolites, from which the template was removed by calcination of the as-synthesized beta zeolite in a stream of ammonia and oxygen, respectively. It has been found that the $CoNH_4$-beta zeolites in contrast to CoH-beta zeolites exhibit high and stable activity in selective catalytic reduction of NO_x with propane in the presence of water vapor (10%). To analyze the reasons for the exception activity of $CoNH_4$-beta zeolites, both zeolite preparations were studied with respect to the state and location of aluminum, character of Al-related acid sites, and Co ion-exchange capacity by means of FTIR spectra of OH groups of dehydrated zeolites and those after adsorption of d_3-acetonitrile, and by ^{29}Si, ^{27}Al, and ^{27}Al 3Q MAS NMR spectra. The procedure of template removal using ammonia provides a charge balance of the framework by NH_4^+ ions and thus preserves framework T–O bonds from perturbation and dealumination. The Co-beta zeolite with high concentrations of regularly Td coordinated Al atoms in the framework ($CoNH_4$-BEA) contains besides the "bare" Co ions the Co ion species adjacent to a single framework Al atom, which moreover, do not adsorb base molecules. These Co species are expected to bear extraframework oxygen(s), and they are suggested to be responsible for the high and stable SCR-NO_x activity at a high content of water vapor in the reactant stream, as their concentration correlates with the C_3H_8–SCR-NO_x activity under water vapor presence.

Keywords: Co-beta; SCR-NO_x; Al distribution in zeolites; ^{27}Al NMR; ^{29}Si NMR; IR spectra; Co(II) ions; Co(II) UV–vis spectra

1. Introduction

Co zeolites of ZSM-5 and ferrierite structures with exchanged Co ions exhibit high activity in CH_4–, C_3H_8– and i-C_4H_{10}–SCR-NO_x without the presence of water, but at high concentrations of water vapor, such as exists in real exhaust gases of lean-burn combustion processes, a substantial decrease in activity occurs [1,2]. This loss of activity is predominantly caused by adsorption of water molecules on the Co ions [3]. Recently, Co-beta zeolite with 100% of Co ion exchange has been reported by EniTecnologie and Osaka Gas researchers to possess high and stable activity in C_3H_8–SCR-NO_x at simulated exhaust gas compositions containing water vapor (9%) and SO_2 (150 ppm) [4–6]. The Co-oxo species in Co-beta, monitored by Raman spectra, were suggested to be the active sites of the C_3H_8–SCR-NO_x reaction [7,8]. However, their concentration was estimated to be rather low, below 10% of the total Co concentration. Therefore, we have attempted to obtain further information necessary for understanding the structure of the Co ion species in beta zeolite exhibiting exceptional activity, and to specify preparations of Co-beta zeolites yielding highly active catalyst for real exhaust gases containing water vapor.

Generally, the state, location, and degree of cation exchange in zeolites depend on both the distribution of aluminum in the framework [2,9,10] and the structure of cation

* Corresponding author.
E-mail address: wichterl@jhinst.cas.cz (B. Wichterlová).

0021-9517/$ – see front matter
doi:10.1016/j.jcat.2004.08.001

complexes present in aqueous solutions or in the gas phase during high-temperature "solid-state" ion exchange. Positions and state of the exchanged cations in dehydrated zeolites are affected by the zeolite structure, Al distribution in the framework, and gaseous atmosphere, both providing surrounding—ligand field—for the cation. Cobalt as well as other divalent cations can be present in pentasil-ring zeolites as (i) "bare" cations at cationic sites coordinated exclusively to the framework oxygen atoms and thus exhibiting an open coordination sphere, (ii) oxo- or μ-peroxo Co species coordinated to the framework oxygens and simultaneously bearing extraframework oxygen atom(s), and (iii) various undefined Co oxide-like species (CoO, Co_3O_4) supported in the zeolite inner volume or at the outer surface of the crystals [2,11].

In contrast to zeolites of ZSM-5 and ferrierite structures, the framework of zeolite beta is usually perturbed in the surrounding aluminum atom [12,13]. Some of these perturbations result in the reversible change of the coordination of aluminum atoms in the zeolite framework. There is a general agreement that some framework Al atoms can exhibit octahedral coordination [12,14–20]. The extent of this perturbation depends on the type of the cation balancing the negative charge of the framework and thus also on the conditions under which the template is removed from the as-synthesized zeolite [21]. Generally, if a counterion is represented by a proton, considerable weakening of the framework Al–O bonds occurs, Al atom cans exhibit octahedral coordination, and the framework is substantially perturbed up to the stage of its dealumination [21]. Such dealumination affects thereafter the aluminum distribution within the framework. On the contrary, metal and ammonium ions as counterions stabilize aluminum coordination in AlO_4 tetrahedra in the framework. It follows that the distribution of aluminum between the framework and the extraframework sites can be substantially different depending on the treatment of beta zeolite and type of the counterions balancing the framework.

Framework perturbations leading to changes in aluminum state and its distribution in beta zeolites understandably affect siting and coordination of the exchanged Co ions, which might then be reflected in the activity of Co-beta zeolites. Therefore, we have been interested in the catalytic behavior of Co-beta zeolite catalysts prepared from the parent as-synthesized beta zeolites from which the template was removed by different ways, i.e., by calcinations in an oxygen (standard procedure) or ammonia stream, thus providing a charge balance of the framework by protons or ammonium ions. The template removal in an ammonia stream was first reported by Creyghton et al. [21] and subsequently adopted by other groups.

The study describes the state of aluminum and Al-related acid sites and replacement of the individual acid sites by the Co ions in two different beta zeolites, i.e., H-beta and NH_4-beta, prepared by calcinations of the as-synthesized beta zeolite in an oxygen and ammonia stream, respectively. The activity of the corresponding Co-beta zeolites is compared in selective catalytic reduction of NO_x with propane (C_3H_8–SCR-NO_x) under the presence and absence of water vapor. A high aluminum density in the framework of NH_4-beta zeolite is stressed to play a decisive role for the high and stable catalyst activity in C_3H_8–SCR-NO_x under the presence of water vapor.

2. Experimental

2.1. Parent zeolites

Beta zeolite with $Si/Al_{total} = 11.5$ containing template was supplied by Unipetrol Inc., CZ. Two different procedures were employed for template removal, which resulted in parent H-BEA and NH_4-BEA zeolites, where H^+ and NH_4^+ ions, respectively, balanced the framework charge of zeolites.

H-BEA was prepared by calcination of the as-synthesized beta zeolite with template in an oxygen stream at 450 °C for 24 h (1 °C min^{-1} up to 100 °C, 100 °C for 1 h, 1 °C min^{-1} up to 250 °C, and 5 °C min^{-1} up to 450 °C). Afterward, the zeolite was hydrated in air at room temperature (RT). NH_4-BEA was prepared by calcination of beta zeolite with template in an ammonia stream at 450 °C for 8 h (temperature program as for H-BEA). Then the NH_4 zeolite was exchanged into the Na^+ form by repeated (3×) Na^+ ion exchange using 0.5 M $NaNO_3$ (40 ml per 1 g of a zeolite) at RT. Na-BEA was calcined in an oxygen stream at 450 °C for 24 h to remove rest of the template. Na-BEA zeolite was then ion-exchanged (4×) using 0.2 M NH_4NO_3 (60 ml per 1 g of a zeolite) at RT to guarantee complete exchange by NH_4^+ ions. After washing of the zeolite by distilled water it was dried in air at RT; the resulting zeolite is denoted as NH_4-BEA.

Na forms of the final parent NH_4-BEA and H-BEA zeolites, prepared for NMR studies, were ion-exchanged (3×) with 0.5 M $NaNO_3$ (40 ml per 1 g of a zeolite) at RT. The zeolites were denoted as Na(NH_4)-BEA and Na(H)-BEA, respectively. The procedure yields the maximum concentration of exchangeable Na^+ ions.

The chemical composition of parent zeolites was determined by atomic absorption spectrometry after dissolution of the zeolite samples (Table 1).

Table 1
Composition of parent beta zeolites from chemical analysis

Zeolite	Si/Al_{total}	Na/Al_{total}
BEA-TEA	11.5	–
H-BEA	11.5	–
Na(H)-BEA	13.2	0.43
NH_4-BEA	11.7	–
Na(NH_4)-BEA	11.7	0.70

Al_{total} is obtained from chemical analysis.

Table 2
Composition of Co-beta zeolites and conditions of Co(II) ion exchange

Zeolite	Si/Al_{total}	Co/Al_{total}	Conditions of ion exchange		
			$Co(NO_3)_2$ conc. (mol/L)	Solution/zeolite (ml/g)	Time (h) × repetition
$CoNH_4$-BEA	12.2	0.02	0.0013	75	7
$CoNH_4$-BEA	12.4	0.19	0.0025	75	7
$CoNH_4$-BEA	12.2	0.21	0.0028	75	7
$CoNH_4$-BEA	12.0	0.29	0.0061	75	7
$CoNH_4$-BEA	12.0	0.30	0.0064	75	7
$CoNH_4$-BEA	12.3	0.34	0.0080	75	7
$CoNH_4$-BEA	11.9	0.48	0.05	120	24 × 3
$CoNH_4$-BEA	11.9	0.50	0.05	120	24 × 3
CoH-BEA	13.6	0.08	0.0014	75	7
CoH-BEA	14.0	0.09	0.0046	75	7
CoH-BEA	13.0	0.09	0.0064	75	7
CoH-BEA	14.0	0.22	0.0082	75	7
CoH-BEA	13.1	0.32	0.05	120	24 × 3

2.2. Co zeolites

$CoNH_4$-BEA and CoH-BEA zeolites with various Co concentrations were prepared by Co(II) ion exchange of the corresponding parent beta zeolites with $Co(NO_3)_2$ aqueous solutions at RT. After the Co(II) ion exchange, the zeolites were washed three times with distilled water and dried in air at RT. Detailed parameters of Co(II) ion exchange and chemical compositions of zeolites, determined by atomic absorption spectrometry after the zeolite samples dissolution, are given in Table 2.

2.3. Nuclear magnetic resonance

^{29}Si, ^{27}Al MAS NMR and ^{27}Al 3Q MAS NMR experiments were carried out on a Bruker Avance 500 MHz (11.7 T) wide-bore spectrometer operating at Larmor frequency 130.3 MHz for aluminum and 99.35 MHz for silicon using 4 mm o.d. ZrO_2 rotors.

^{29}Si MAS NMR high-power decoupling (HPDec) and cross-polarization (CP) experiments were carried out. In the case of high-power decoupling, $\pi/6$ (1.7 μs) excitation pulse and 30 s relaxation delay were applied. In the case of cross-polarization spectra, pulse sequences with 50% ramp CP pulse, 2000 μs contact time, high-power decoupling, and 5 s relaxation delay were applied. Rotors were spun at a rotation speed of 5 kHz. ^{29}Si high-power decoupling spectra were decomposed to the Gaussian bands using Microcall Origin 4.1 software (Microcall Software Inc., USA). Framework aluminum content (Si/Al_{FR}) was estimated according to formula

$$Si/Al_{FR} = I/0.25I_1, \tag{1}$$

where I_1 denotes the intensity of the NMR line corresponding to the Si(3Si,1Al) building unit, and I denotes total ^{29}Si intensity; for details see Ref. [22].

To enable quantitative analysis of ^{27}Al MAS NMR spectra, high-power decoupling pulse sequences with $\pi/12$ (0.7 μs) excitation pulse and 1 s relaxation delay were applied on fully hydrated samples. Rotors were spun at rotation speed of 12 kHz and chemical shifts were referenced to the aqueous solution of $Al(NO_3)_3$. Spectra were normalized to the weight of the sample and decomposed to the Gaussian bands using Microcall Origin. ^{27}Al 3Q experiments were performed using the two-pulse z-filtered procedure. A π pulse was used for excitation and a $\pi/3$ pulse for conversion. Pulses were individually optimized for each sample. Relaxation delay was 0.5 s. 2D contour plots presented are the results of a 2D Fourier transformation followed by a shearing transformation. Thus, the F1 axis is the isotropic dimension and F2 gives the MAS spectrum containing the second-order quadrupolar lineshape. Isotropic chemical shift and second-order quadrupolar parameters were obtained from the first moment analysis of the 2D plot using the following relations

$$\delta_{iso} = (17\delta_{F1} + 10\delta_{F2})/27 \tag{2}$$

and

$$P_Q = C_{QCC}(1+\eta^2/3)^{1/2} = \left((17/162\,000)\nu_L^2(\delta_{F1}-\delta_{F2})\right)^{1/2}, \tag{3}$$

where ν_L is the Larmor frequency. For a discussion of ^{27}Al 3Q MAS in beta zeolites, see Refs. [13,23]; for details on 3Q MAS NMR see Refs. [24,25].

2.4. FTIR spectroscopy

FTIR spectra in the region of OH groups and C≡N vibrations were monitored at RT on parent and Co-beta samples after evacuation (10^{-3} Pa) at 450 °C and after adsorption of d_3-acetonitrile (10 Torr at RT) followed by its desorption at RT and at 150 °C for 20 min in a glass vacuum cell equipped with NaCl windows and a carousel sample holder with six samples. FTIR spectrometer Nicolet Magna-550 with a MCT-B low-temperature detector was used. For a single spectrum, 200 scans at 2 cm^{-1} resolution were collected. Samples were used as self-supported pellets of thickness of about 5 mg cm^{-2}. Spectra intensities were normalized on the

sample thickness using the integral area of the zeolite skeletal bands. Concentration of unperturbed bridging OH groups (OH, IR band at 3610 cm^{-1}), Brønsted sites representing the sum of the unperturbed and perturbed bridging OH groups (BS, band at 2297 cm^{-1} of C≡N vibrations), Al-Lewis sites (LS, band at 2325 cm^{-1} of C≡N vibrations), and Co-Lewis sites adsorbing d_3-acetonitrile (Co_A, band at 2308 cm^{-1} of C≡N vibrations) were determined by using extinction coefficients $\varepsilon_{OH} = 4.05 \pm 0.21$ [26], $\varepsilon_B = 2.05 \pm 0.10$ [26], $\varepsilon_L = 3.62 \pm 0.16$ [26], $\varepsilon_{Co} = 7.12 \pm 0.35$ [27]. The amount of NH_4^+ ion was determined in hydrated NH_4-BEA sample from the band at 1445 cm^{-1} and extinction coefficient $\varepsilon_{NH} = 13.0 \pm 0.6$ cm µmol^{-1} [28]. Details of the applied IR procedure are given in Refs. [29,30].

2.5. Selective catalytic reduction of NO_x with propane

C_3H_8–SCR-NO_x over parent and Co-beta zeolites was carried out in a glass flowthrough microreactor, typically with 400 mg of the catalyst. The reactor inner volume was filled with glass balls to minimize conversion of C_3H_8 in the gaseous phase prior to the catalyst bed. Reactant mixture consisting of 1000 ppm NO, 1000 ppm C_3H_8, 2.5% O_2, 0 or 10% H_2O, and the rest of He was kept at a total flow of 100 ml min^{-1}. Corresponding GHSV was 7500 h^{-1}, assuming a specific catalyst density of 0.5 g cm^{-3}.

The catalyst was pretreated in an oxygen stream at 450 °C for 1 h (5 °C min^{-1}). During this procedure NH_4 zeolites were deammoniated to H zeolites under in situ conditions. After calcination of the catalyst the reactor was cooled to the lowest reaction temperature, typically 200 °C, kept constant, and connected with a reactant stream. The steady state of the reaction was usually reached within 30–50 min. C_3H_8–SCR-NO in the absence of water vapor was measured from 200 to 450 °C at temperature steps of 50 °C. The effect of water addition to the reaction stream on the zeolite activity was measured at 350 °C.

Concentrations of NO and NO_2 in the inlet and outlet of the reactor were continuously monitored by an NO/NO_x chemiluminescence analyzer (VAMET-CZ). Concentrations of C_1–C_3 hydrocarbons, CO_2, CO, and N_2O were provided by an on-line connected Hewlett Packard 6090 gas chromatograph. Two gaseous samples were simultaneously injected. In one branch, columns of Poraplot Q (30 m × 0.53 mm) and Molecular sieve 5 A (30 m × 0.53 mm, d_f = 25 µm) were used for separation of CO_2, CO, and N_2O (TCD detector). A by-pass with Molecular sieve 5 A column was used for analysis of CO_2. In the second branch, a FID detector monitored C_1–C_3 hydrocarbons separated on a nonpolar HP-5 column (30 m × 0.32 mm with 0.25 µm thickness of active phase). When the reaction was carried out with 10% H_2O in the feed, an ice-cooled water trap (4 °C) was used to reduce water vapor pressure at the outlet of the reactor prior to the NO/NO_x and GC analysis of reactants and products.

Conversion of the reactant i, i.e., NO or C_3H_8 was defined as

$$x_i\ (\%) = \frac{c_i^0 - c_i}{c_i^0} \times 100 \tag{4}$$

where c_i^0 is the concentration [ppm] of the reactant i in the feed, and c_i is the concentration of the reactant i after the reaction.

Yields of NO_2 and N_2O related to NO and yields of CO_2, CO, CH_4, C_2H_6, C_2H_4, and C_3H_6 related to C_3H_8 were defined as

$$y_j\ (\%) = \frac{v_j c_j}{v_i c_i^0} \times 100, \tag{5}$$

where c_j is the concentration [ppm] of the product j, i.e., NO_2, N_2O, CO_2, CO, CH_4, C_2H_6, C_2H_4, or C_3H_6, in the reactor outlet, and v_j is the number of C or N atoms in the corresponding molecule, c_i^0 is the concentration [ppm] of the reactant i, i.e., NO or C_3H_8, in the reactor inlet, and v_i is the number of C or N atoms in the corresponding molecule.

N_2 yield was calculated according to

$$y_{N_2}\ (\%) = x_{NO} - (y_{NO_2} + y_{N_2O}) \tag{6}$$

as other N-containing compounds were not found in the product mixture. The values of N_2 yield calculated from the N balance were confirmed by gas chromatographic analysis. Turnover-frequency values (TOF, h^{-1}) represent molecules of NO converted to N_2 per Co atom per hour.

3. Results

3.1. Structure of Al-related acid sites of parent H- and NH_4-beta zeolites

3.1.1. FTIR spectra

Fig. 1 shows FTIR spectra of adsorbed d_3-acetonitrile on deammoniated/dehydrated NH_4-BEA and H-BEA zeolites in the region of C≡N vibration. Bands at 2325

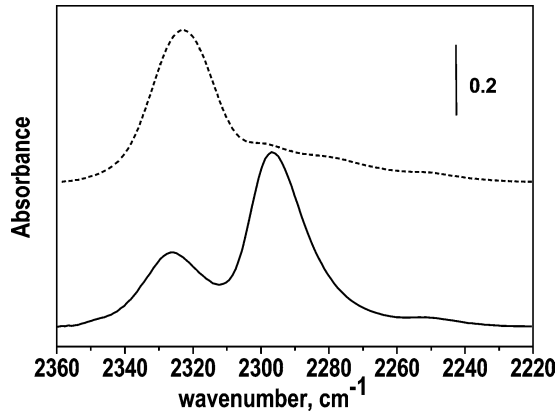

Fig. 1. FTIR spectra of deammoniated/dehydrated (450 °C) NH_4-BEA (—) and H-BEA (- - -) after adsorption of d_3-acetonitrile at RT.

Table 3
Content of Al from chemical analysis, IR and NMR spectra of parent beta zeolites

Zeolite	Si/Al_{total}	Content of Al (mmol g^{-1})							
		Al_{total}	NH_4^+	OH	Brønsted sites (BS)	Lewis sites (LS)	Al_{IR}	Si/Al_{FR} [a]	Al_{NMR} [b]
H-BEA	11.5	1.33	–	0.07	0.24	0.49	1.22	–	–
Na(H)-BEA	13.2	1.17	–	n.d.	n.d.	n.d.	n.d.	20.3	0.78
NH_4-BEA	11.7	1.31	1.22	0.38	0.78	0.25	1.28	–	–
Na(NH_4)-BEA	11.7	1.31	–	n.d.	n.d.	n.d.	n.d.	13.0	1.19

[a] Determined by ^{29}Si NMR, see Table 4.
[b] Calculated from Si/Al_{FR}.

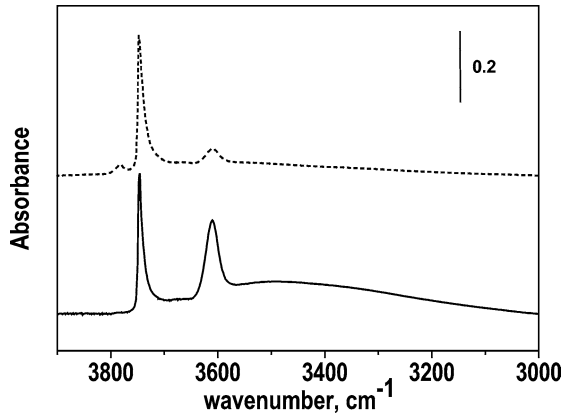

Fig. 2. FTIR spectra of NH_4-BEA (—) and H-BEA (- - -) dehydrated/deammoniated at 450 °C.

and 2297 cm^{-1} reflecting the interaction of C≡N group with Lewis and Brönsted sites, respectively, were found in the spectra of both samples. The intensity of the band at 2325 cm^{-1} highly prevailed in the spectra of H-BEA compared to NH_4-BEA, where the intensity of the band at 2297 cm^{-1} was much higher compared to that at 2325 cm^{-1}. Thus, H-BEA exhibited predominantly Lewis sites compared to very low concentrations of Brönsted sites, while with the NH_4-BEA sample the concentrations of Brönsted sites highly prevailed over that of Lewis sites (see Table 3).

Fig. 2 shows FTIR spectra of NH_4-BEA and H-BEA deammoniated/dehydrated at 450 °C in the region of OH vibrations. A band at 3610 cm^{-1} characteristic for unperturbed bridging Si–OH–Al groups [12,14,31], i.e., not affected by hydrogen bonding with the other OH groups, and a band at 3745 cm^{-1} characteristic for terminal Si–OH groups were found in the spectra of both zeolites [12,14,31]. FTIR spectrum of H-BEA exhibited in addition a band at 3780 cm^{-1} ascribed to OH groups bound to framework Al in defective sites with adjacent Si–OH groups [12,14], and a low-intensity band at 3660 cm^{-1} ascribed to OH groups bound to extraframework aluminum [12]. Both these species exhibit a Lewis character. Besides the bands at 3610 and 3745 cm^{-1}, the spectrum of NH_4-BEA exhibited a broad band ranging from ca 3700 and 3200 cm^{-1}, which was attributed in the literature to the bridging OH groups perturbed via hydrogen bonding with the other bridging OH or silanol groups [12,31,32]. In NH_4-BEA, this band represented mostly hydrogen bonding between two close bridging OH groups [33].

There is a good agreement between the concentrations of Al in zeolites calculated from chemical analysis (Al_{total}) and those determined from the IR spectra (Al_{IR}, the sum of concentrations of Brönsted sites and twice those of Al-Lewis sites) for both NH_4-BEA and H-BEA zeolites (Table 3). It implies that all Al sites with an open coordination sphere in the deammoniated/dehydrated zeolites were detected by adsorbed d_3-acetonitrile as Lewis sites, i.e., that no clustering of these species occurred. With the hydrated NH_4-BEA sample the concentration of NH_4^+ ions was determined from the intensity of the band of N–H vibrations at 1445 cm^{-1}, NH_4^+ [28]. As this value (1.22 mmol NH_4^+ g^{-1}) matched satisfactorily the chemical analysis of aluminum (1.31 mmol Al g^{-1}), it follows that the hydrated NH_4-BEA zeolite contained Al atoms predominantly in the framework positions.

3.1.2. NMR spectra

The spectra were monitored on the both parent NH_4-BEA and H-BEA zeolites and their sodium forms. ^{29}Si single pulse MAS NMR spectra of Na(NH_4)-BEA and Na(H)-BEA are shown in Fig. 3A, and corresponding CP spectra are given in Fig. 3B. No difference was observed between ^{29}Si NMR spectra of parent zeolites (NH_4- and H-) and corresponding Na forms. Decomposition of the single pulse spectra to the Gaussian bands is depicted in Fig. 4 and the results are summarized in Table 4. As follows from Figs. 3 and 4, a single pulse spectrum is composed from 6 bands with maxima at −115.0, −110.8, −104.8, −103.0, −101.1, and −95.5 ppm. A band around 98.0 ppm, attributed to Si(2Si,2Al) [16,34], was not observed. Because the intensity of the resonance at −101.1 and −95.5 ppm significantly increased in the cross-polarization spectrum (see Fig. 3B), both bands can be attributed to the Si–OH species. The bands at −104.8 and −103.0 ppm correspond to Si(3Si,1Al) and the bands at −115.0 and −110.8 ppm to Si(4Si); cf. Ref. [22].

Using the above given attribution of ^{29}Si NMR bands to the Si(Si,Al) species and the areas of these bands (Table 4 and Eq. (1)), the content of framework aluminum in zeolites was estimated; see Table 3 (Na(NH_4)-BEA 1.19 mmol Al g^{-1}, Si/Al_{FR} = 13.0 and Na(H)-BEA 0.78 mmol Al g^{-1}, Si/Al_{FR} = 20.3). Note that the value of Si/Al_{FR} = 13.0 fits well with that obtained from chemical analysis.

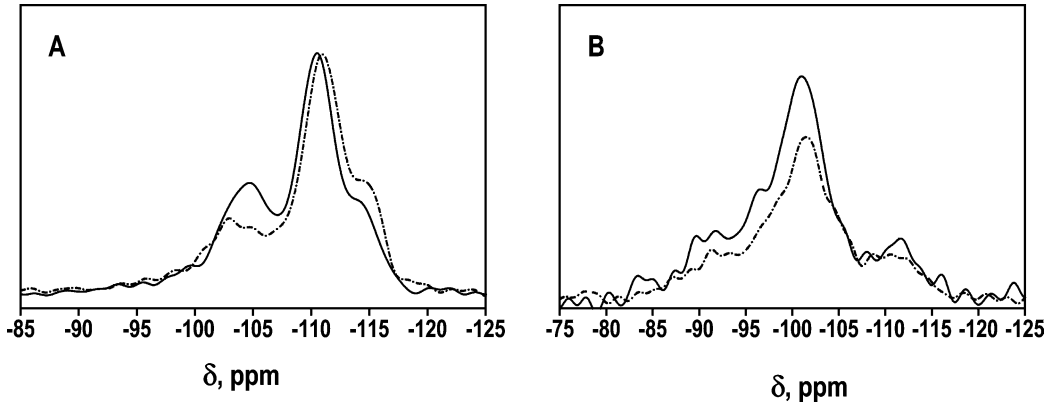

Fig. 3. ^{29}Si MAS NMR (A) single pulse and (B) CP spectra of Na(NH_4)-BEA (—) and Na(H)-BEA (-·-).

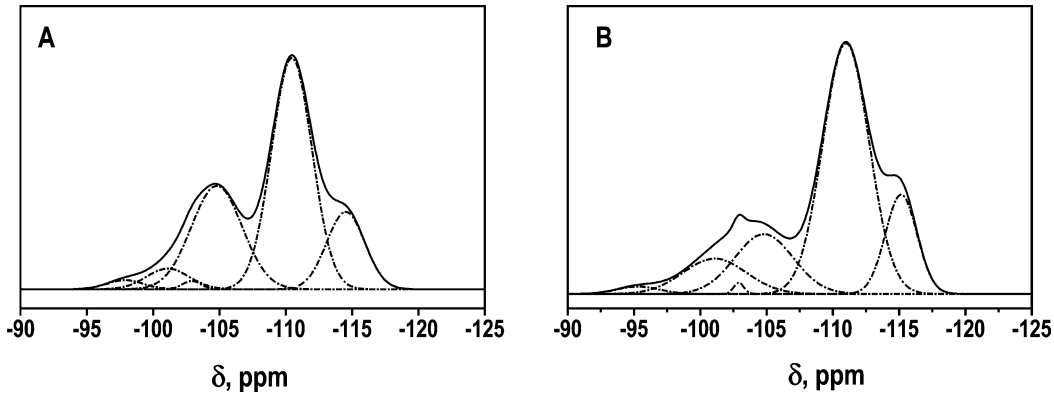

Fig. 4. Simulation of ^{29}Si single pulse MAS NMR spectra of (A) Na(NH_4)-BEA and (B) Na(H)-BEA.

Table 4
NMR parameters and relative intensities of ^{29}Si MAS NMR spectra

Zeolite	δ (ppm)/intensity (a.u.)					
Na(NH_4)-BEA	−114.6/15	−110.5/49	−104.8/28	−102.9/1	−101.1/5	−95.5/2
Na(H)-BEA	−115.1/15	−110.9/55	−104.8/16	−102.9/1	−101.1/11	−95.5/2

As follows from Fig. 3 and Table 4, the differences in the treatment of template removal with Na(NH_4)-BEA and Na(H)-BEA caused a significant decrease of the intensity of the band at −104.8 ppm (Si(3Si,1Al)), which was lower for Na(H)-BEA, while the intensity of the band at −101.1 (Si–OH) increased. This is clearly seen in the subtraction of the spectra of Na(H)-BEA and Na(NH_4)-BEA. Changes in the intensity of the bands at −104.8 and −101.1 ppm evidence the dealumination of the framework accompanied by the defect formation.

^{27}Al MAS NMR spectra of NH_4-, Na(NH_4), H-, and Na(H)-BEA zeolites are depicted in Fig. 5A; details of the region of Td coordinated Al are given in Fig. 5B. NMR signal around 0 ppm corresponding to the octahedrally coordinated aluminum was observed only with H-BEA sample. Two Oh-coordinated Al species represented by a sharp transition at 0 ppm and broad one centered at −8 ppm were identified. Two resonances with chemical shifts of 57.5 and 54.0 ppm are present in the spectrum of H-BEA sample and

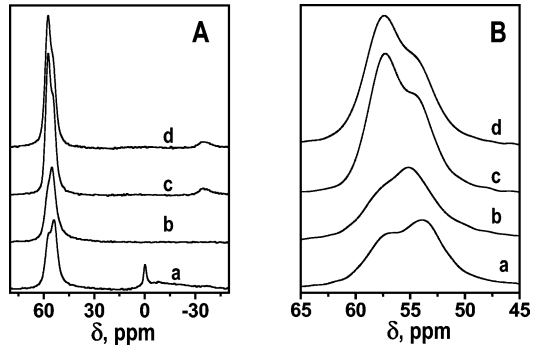

Fig. 5. ^{27}Al MAS NMR spectra of (a) H-BEA, (b) Na(H)-BEA, (c) NH_4-BEA, and (d) Na(NH_4)-BEA.

two resonances at 57.5 and 55.1 ppm belong to NH_4-BEA zeolite and to Na forms of both parent zeolites. The resonance at 57.5 ppm predominates in the spectrum of NH_4- and Na(NH_4)-BEA, while in the case of Na(H)-BEA, the resonance at 55.1 ppm prevails. Resonance at 54.0 ppm pre-

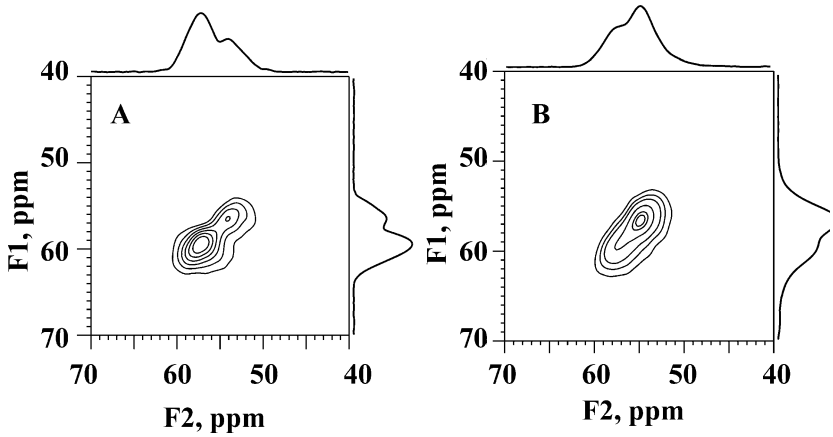

Fig. 6. ^{27}Al 3Q MAS NMR spectra of (A) Na(NH_4)-BEA and (B) Na(H)-BEA.

Table 5
NMR parameters of ^{27}Al 3Q MAS NMR spectra

Zeolite	Al(IV)-A		Al(IV)-B	
	δ_{iso} (ppm)	P_Q (MHz)	δ_{iso} (ppm)	P_Q (MHz)
Na(NH_4)-BEA	58.7	1.98	55.2	1.79
Na(H)-BEA	58.7	1.74	56.2	1.74

vails with H-BEA. The intensity of the ^{27}Al MAS NMR signal of NH_4-, H-, and Na(NH_4)-BEA zeolites reached the same values, while the intensity of the signal of the Na(H) zeolite reached only 65% of the intensity of NH_4 zeolite.

Only Na forms of BEA zeolites can be employed to monitor the distribution of Al atoms within framework T sites (see Discussion); they were investigated using the 3Q experiment. Fig. 6A shows the ^{27}Al 3Q MAS NMR spectrum of Na(NH_4)-BEA. Two types of Al(IV) resonances with isotropic shift 58.7 ppm (Al(IV)-A) and 55.5 ppm (Al(IV)-B) are present in the spectrum. Fig. 6B shows the ^{27}Al 3Q MAS NMR spectrum of Na(H)-BEA. The intensity of the resonance of Al(IV)-A species is lower compared to that of Na(NH_4)-BEA and the Al(IV)-B species with isotropic shift of 56.2 ppm predominates in the spectrum. The NMR parameters of both Al species obtained according to Eqs. (2) and (3) are given in Table 5.

As the MAS NMR spectra show negligible quadrupolar broadening, the single pulse spectra were deconvoluted using Gaussian lineshapes and the relative intensities obtained for the individual resonances are listed in Table 5. It is to be noted that the total ^{27}Al NMR intensity was lower with Na(H)-BEA and represents only 65% of the ^{27}Al intensity of the Na(NH_4)-BEA sample.

3.2. Co ion exchange

FTIR spectra were used to follow the exchange of the individual Al-related acid sites by Co(II) ions in NH_4-BEA and H-BEA zeolites. Fig. 7 shows the dependence of the concentrations of unperturbed bridging Si–OH–Al groups (OH, 3610 cm^{-1}), Brönsted sites (BS, 2297 cm^{-1}), i.e., sum

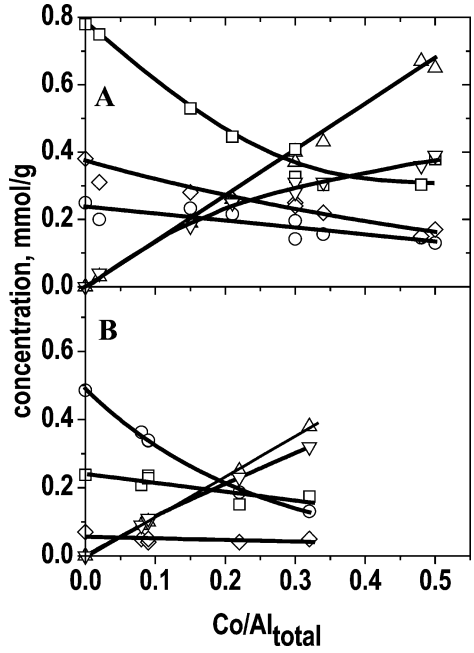

Fig. 7. Dependence of the concentration of Brønsted sites (□), Al-Lewis sites (○), unperturbed bridging OH groups (◇), Co ions interact with d_3-acetonitrile (▽) and total amount of Co(II) ions (△) on Co/Al$_{total}$ in (A) CoNH$_4$-BEA and (B) CoH-BEA zeolites.

of the unperturbed and perturbed bridging OH groups, Al-Lewis sites (LS, 2325 cm^{-1}), Co sites interacting with d_3-acetonitrile (Co$_A$, 2308 cm^{-1}), and the concentration of Co ions determined by chemical analysis (Co$_{total}$) on Co/Al$_{total}$ molar ratio in NH_4-BEA (Fig. 7A) and H-BEA (Fig. 7B). However, it should be noted that the bands of adsorbed d_3-acetonitrile on Brönsted (2297 cm^{-1}) and Co (2308 cm^{-1}) sites strongly overlap and, therefore, the concentrations of Brönsted and Co sites represent a rough estimate especially for samples with Co/Al > 0.3.

The increasing Co(II) ion exchange into NH_4-BEA caused a sharp decrease in the concentration of Brönsted sites (Fig. 7A). The decrease in concentration of these sites was much higher than the decrease in the concentration of

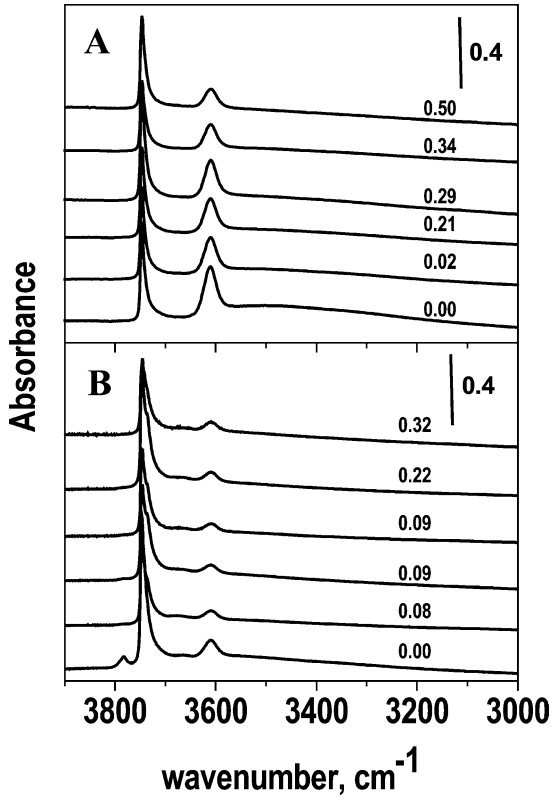

Fig. 8. FTIR spectra in the region of OH vibrations of deammoniated/dehydrated Co-zeolites with different Co/Al_{total} ratio for (A) $CoNH_4$-BEA and (B) CoH-BEA zeolites.

unperturbed bridging Si–OH–Al groups up to Co/Al_{total} ca. 0.3. This indicates, that the Co(II) ions were predominantly exchanged at perturbed close bridging Si–OH–Al groups. These findings are in agreement with a disappearance of the broad band between 3750 and 3200 cm^{-1} reflecting the perturbed bridging Si–OH–Al groups (Fig. 8A) and a low decrease in the intensity of the unperturbed Si–OH–Al groups at 3610 cm^{-1}. A decrease in the relatively low concentration of Lewis sites with increasing degree of Co ion exchange was not high.

On the contrary, the Co(II) ion exchange into H-BEA resulted in a sharp decrease in the high concentration of Lewis sites in the parent zeolite (Fig. 7B) and immediate disappearance of the band at 3780 cm^{-1} of Al–OH groups bound to the framework at perturbed sites (Fig. 8B). The exchange was accompanied by only a small decrease in the concentration of Brönsted sites and the low concentration of unperturbed Si–OH–Al groups was not changed. This indicates that in the H-BEA zeolite the Co(II) ions were at first exchanged at cationic sites, where perturbation of the framework occurred if protons balanced the negative framework charge.

The differences in the parent NH_4-BEA and H-BEA zeolites with respect to aluminum concentration and distribution in the framework were also manifested in a different maximum concentration of the Co(II) ions incorporated into the zeolites. While with NH_4-BEA a complete Co ion exchange related to Al_{total} was obtained ($Co/Al_{total} = 0.50$, $Co/Al_{FR} = 0.54$, see Table 6), with the H-BEA zeolite, due to framework dealumination, the concentration of Co(II) ions was lower, with values of $Co/Al_{total} = 0.32$ corresponding to $Co/Al_{FR} = 0.48$ (see Table 6; $Si/Al_{FR} = 20.3$ for H-BEA calculated from the NMR spectra). Note that with CoH-BEA practically all the Co ions adsorbed d_3-acetonirile, while with $CoNH_4$-BEA zeolites with $Co/Al_{total} > 0.3$, a considerable part of Co species did not interact with d_3-acetonitrile (Co_{NA}, see Fig. 7A and Table 6, difference in the concentrations of Co ions given by chemical analysis and those obtained from the intensity of the IR band at 2308 cm^{-1}).

3.3. Selective catalytic reduction of NO by propane in the absence of water vapor

Figs. 9 and 10 depict the dependence of N_2 yield (A) and C_3H_8 conversion (B) on temperature in C_3H_8–SCR-NO in the absence of water vapor over $CoNH_4$-BEA and CoH-BEA zeolites possessing different Co concentrations. N_2 yields and C_3H_8 conversions for parent H-BEA and NH_4-BEA zeolites reflect the presence of trace concentrations of Fe (300 ppm Fe) and the presence of protonic sites in zeolites; for more information see Refs. [35–37]. With the increasing Co concentration, the increase in the N_2 yield and the shift of its maximum to lower temperatures (accompanied by an increase in C_3H_8 conversion) were observed. The highest N_2 yield exhibited $CoNH_4$-BEA catalyst with maximum level of Co ion exchange; i.e., $Co/Al_{total} = 0.50$. It is difficult to compare and analyze the activity of Co zeolites at low Co loadings, as in this concentration region protonic, Al-Lewis, and trace concentrations of Fe contribute to the catalytic reaction [35–37]. However, if Co zeolites contained high and similar Co concentrations, regardless of the method of preparation of their parent matrices, i.e., $CoNH_4$-BEA ($Co/Al_{total} = 0.30$, $Co/Al_{FR} = 0.31$) and CoH-BEA ($Co/Al_{total} = 0.32$, $Co/Al_{FR} = 0.48$), they exhibited the same temperature profile of NO_x and C_3H_8 conversions.

Yields of CO, CO_2, NO_2, and N_2 in C_3H_8–SCR-NO_x without water vapor in the feed over $CoNH_4$-BEA with Co/Al_{total} 0.50 and CoH-BEA with Co/Al_{total} 0.32 ($Co/Al_{FR} = 0.48$) on temperature are given in Figs. 11A and B. Only very low yields of NO_2 (below 3%) and CH_4, C_2H_4, and C_3H_6 (their sum $< 2\%$) were found. No N_2O, ethane, organic oxygenates, or nitrogen-containing products were detected. While the $CoNH_4$-BEA zeolite with maximum Co(II) concentration produced mainly CO_2, a high yield of undesirable CO was formed over CoH-BEA with maximum Co(II) ions incorporated.

Table 6
Composition of Co-beta zeolites

Zeolite	Si/Al_{total}	Co/Al_{total}	Co/Al_{FR}	Co_{total} (mmol g^{-1})	Co_A [a] (mmol g^{-1})	Co_{NA} [b] (mmol g^{-1})
$CoNH_4$-BEA	12.2	0.02	0.02	0.03	0.05	0
$CoNH_4$-BEA	12.4	0.19	0.20	0.24	0.23	0.01
$CoNH_4$-BEA	12.2	0.21	0.22	0.26	0.25	0.01
$CoNH_4$-BEA	12.0	0.29	0.31	0.37	0.28	0.09
$CoNH_4$-BEA	12.0	0.30	0.32	0.38	0.31	0.07
$CoNH_4$-BEA	12.3	0.34	0.36	0.43	0.31	0.12
$CoNH_4$-BEA	11.9	0.48	0.52	0.62	0.36	0.26
$CoNH_4$-BEA	11.9	0.50	0.54	0.65	0.39	0.26
CoH-BEA	13.6	0.08	0.12	0.09	0.09	0.0
CoH-BEA	14.0	0.09	0.13	0.10	0.10	0.0
CoH-BEA	13.0	0.09	0.15	0.11	0.11	0.0
CoH-BEA	14.0	0.22	0.31	0.25	0.23	0.02
CoH-BEA	13.1	0.32	0.48	0.38	0.30	0.06

[a] Cobalt ions adsorbing d_3-acetonitrile.
[b] Cobalt ions not adsorbing d_3-acetonitrile.

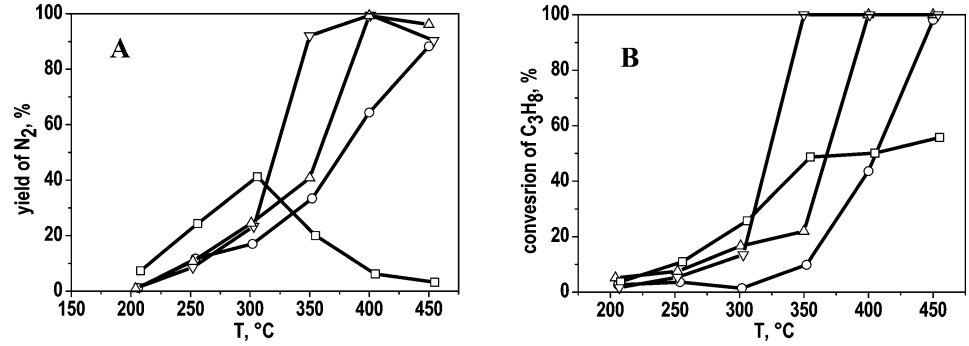

Fig. 9. Dependence of (A) N_2 yield and (B) C_3H_8 conversion in C_3H_8–SCR-NO in the absence of water vapor on temperature over $CoNH_4$-BEA with Co/Al_{total} 0.00 (□), 0.19 (○), 0.30 (△), and 0.50 (▽); 1000 ppm NO, 1000 ppm C_3H_8, 2.5% O_2, and He, GHSV 7500 h^{-1}.

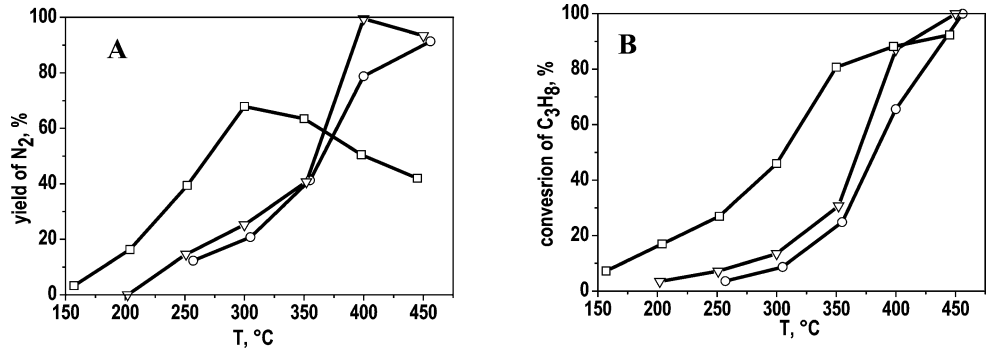

Fig. 10. Dependence of (A) N_2 yield and (B) C_3H_8 conversion in C_3H_8–SCR-NO in the absence of water vapor on temperature over CoH-BEA with Co/Al_{total} 0.00 (□), 0.22 (○) and 0.32 (▽); 1000 ppm NO, 1000 ppm C_3H_8, 2.5% O_2, and He, GHSV 7500 h^{-1}.

3.4. Selective catalytic reduction of NO by propane in the presence of water vapor

Figs. 12 and 13 show the effect of addition of water vapor (10%) in the reactant feed on the activity of $CoNH_4$-BEA and CoH-BEA catalysts at 350 °C, which was completely reversible. While the N_2 yield and C_3H_8 conversion were substantially suppressed in the presence of water vapor with CoH-BEA catalysts, the activity of $CoNH_4$-BEA catalysts was much more resistant to water vapor particularly at high Co loadings. Only small differences between the zeolite activity in the absence and presence of water vapor were observed with $CoNH_4$-BEA catalysts at $Co/Al_{total} > 0.3$. A comparison of the activity of Co zeolites at low cobalt loadings can hardly be done due to different activity and behavior of the sites in parent zeolites.

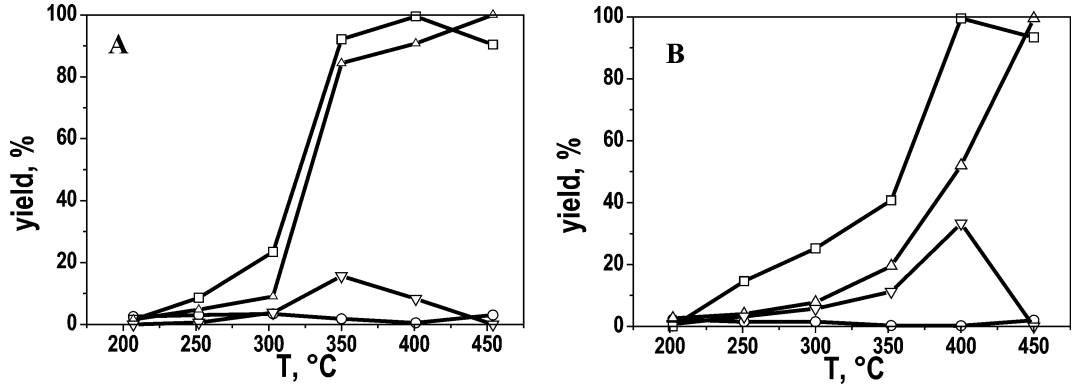

Fig. 11. Dependence of the yields of CO_2 (△), CO (▽), NO_2 (○), and N_2 (□) in C_3H_8–SCR-NO in the absence of water vapor on temperature over (A) $CoNH_4$-BEA with Co/Al_{total} 0.50, (B) CoH-BEA with Co/Al_{total} 0.32. 1000 ppm NO, 1000 ppm C_3H_8, 2.5% O_2, and He, GHSV 7500 h^{-1}.

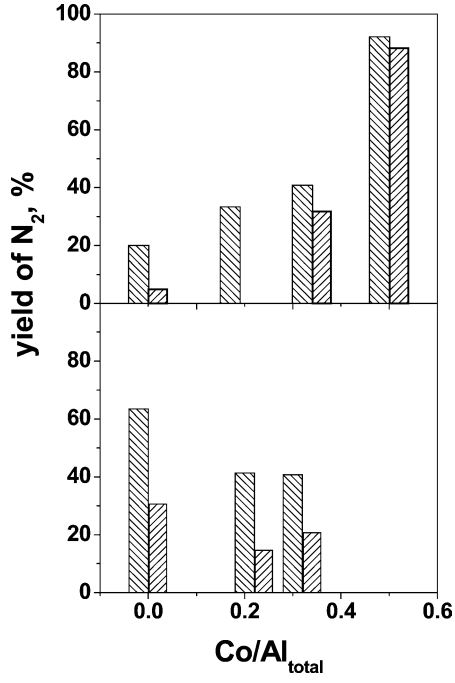

Fig. 12. Dependence of N_2 yield in C_3H_8–SCR-NO at water absence (▨)/presence (▨) on Co/Al_{total} over (A) $CoNH_4$-BEA and (B) CoH-BEA zeolites at 350 °C. 1000 ppm NO, 1000 ppm C_3H_8, 2.5% O_2, 0 or 10% H_2O, and He, GHSV 7500 h^{-1}.

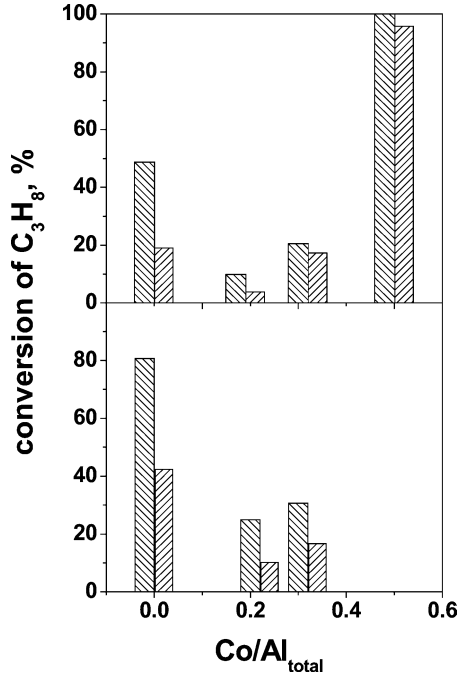

Fig. 13. Dependence of C_3H_8 conversion in C_3H_8–SCR-NO at water absence (▨)/presence (▨) on Co/Al_{total} over (A) $CoNH_4$-BEA and (B) CoH-BEA zeolites at 350 °C. 1000 ppm NO, 1000 ppm C_3H_8, 2.5% O_2, 0 or 10% H_2O, and He, GHSV 7500 h^{-1}.

To test the stable performance of $CoNH_4$-BEA (Co/Al_{total} 0.50) in C_3H_8–SCR-NO, the reaction was carried out also at GHSV 30,000 h^{-1} (Fig. 14) and for time on stream of 90 h (Fig. 15). A minimum difference between the catalyst activity in the reaction carried out in the presence and absence of water vapor was observed also at GHSV 30,000 h^{-1} (Fig. 14). High activity of $CoNH_4$-BEA (Co/Al_{total} 0.50) was stable for ca. 90 h. N_2O was not detected in the products and only low yields of NO_2 (below 2.5%) were found. The catalyst also showed high conversion of C_3H_8 to CO_2 (70%) and only low conversion to CO (18%).

The activity of $CoNH_4$-BEA zeolites in water vapor presence was also compared in turnover-frequency values at 350 °C for conversion of NO to N_2 related to one Co ion (Fig. 16, line a) and to the concentration of Co species not adsorbing acetonitrile (Fig. 16, line b). The TOF values were calculated at 350 °C, as up to this temperature the exponential dependence of N_2 yield vs temperature was followed, although for highly loaded $CoNH_4$-BEA the conversion values were relatively high. Therefore, the TOF values represent a rough estimate. Note that in the presence of water vapor in the reactant stream, the contribution of parent zeolites to the $CoNH_4$-BEA activity is negligible. With the $CoNH_4$-BEA zeolites active in the presence of water vapor, it is clearly seen that with the increasing Co loading TOF values increase linearly per Co ion (total) (Fig. 16, line a), while if TOF values are related to the concentration of Co species not ad-

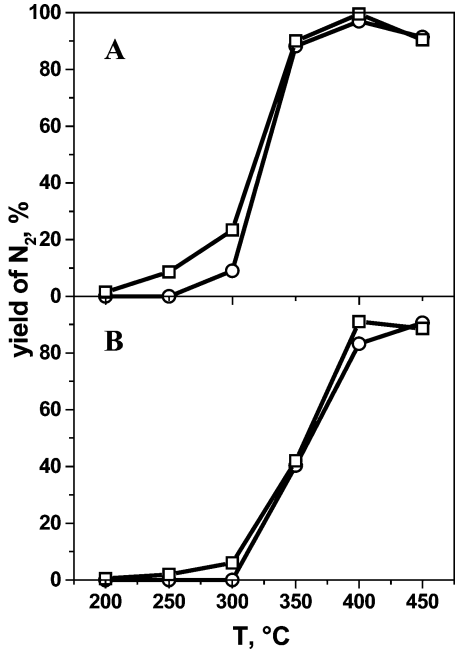

Fig. 14. Dependence of N_2 yield in C_3H_8–SCR of NO on temperature and water presence over $CoNH_4$-BEA with Co/Al_{total} 0.50. 1000 ppm NO, 1000 ppm C_3H_8, 2.5% O_2, 0 (□) or 10% (○)% H_2O, and He, GHSV (A) 7500 and (B) 30,000 h^{-1}.

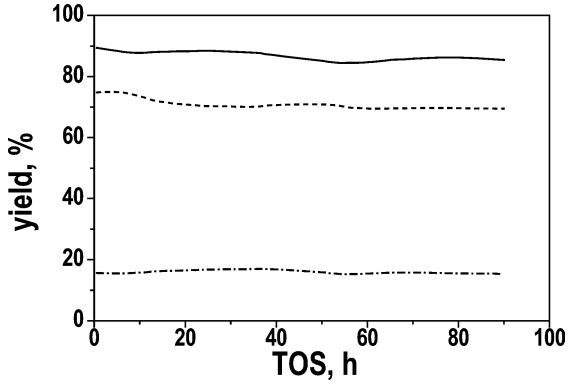

Fig. 15. Dependence of the yields of N_2 (—), CO_2 (- - -) and CO (-·-) in C_3H_8–SCR-NO on time-on-stream over $CoNH_4$-BEA (Co/Al_{total} 0.5) in the presence of H_2O. 1000 ppm NO, 1000 ppm C_3H_8, 2.5% O_2, 10% H_2O, and He, GHSV 7500 h^{-1}.

sorbing acetonitrile (Co_{NA}, Table 6), then constant TOF is obtained (line b).

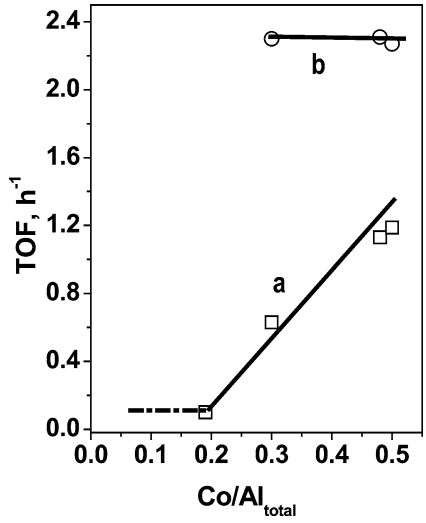

Fig. 16. Dependence of TOF related to one Co ion (line a) and TOF related to the concentration of Co species not adsorbing d_3-acetonitrile (line b) on the Co concentration in C_3H_8–SCR-NO in the presence of water over $CoNH_4$-BEA zeolites at 350 °C.

4. Discussion

4.1. Structure of Al-related acid sites of parent beta zeolite

Contrary to other zeolites, the structure of beta zeolite is connected with a reversible change of the coordination of framework Al atoms. It is generally accepted that at least a part of the framework Al atoms exhibits an octahedral coordination, Oh (in H-BEA), besides a tetrahedral one (Td) depending on the type of a counter ion balancing framework negative charge [14–20]. However, disappearance of the Oh ^{27}Al signal due to sodium exchange of H-BEA was not followed by the intensity increase of the Td signal. The signal intensity of Na(H)-BEA reached only 65% of that of H- or NH_4-BEA samples. Thus, Oh aluminum in H-BEA represents extraframework species. This suggestion is supported by a significant decrease in the framework aluminum content in H- and Na(H) samples compared to NH_4- and Na(NH_4)-BEA evidenced by ^{29}Si NMR. Oh-coordinated aluminum was probably converted during sodium exchange to invisible Al species with an unspecified environment. The concentration of invisible extraframework Al species (35%) is surprisingly high. Nevertheless, such Al species have been recently reported [23]. It is necessary to point out that also the coordination of tetrahedral framework atoms can be affected by the nature of a countercation in the zeolite [38,39]. This follows from the shift of the Td resonance of H- and Na(H)-BEA samples from 54.0 to 55.1 ppm. It implies that the H form of BEA zeolite cannot be employed to check the presence of extraframework Al species and, moreover, to estimate the distribution of framework Al atoms among the T sites. Thus, only Na(H)- and Na(NH_4)-BEA zeolites are useful for investigation of the effect of calcination procedure on the aluminum distribution in the framework.

A lower concentration of Al in the framework of H-BEA zeolite compared to NH_4-BEA is indicated by the ^{29}Si NMR spectrum (Si/Al_{FR} 20.3 vs 13.0), and the lower intensity of the ^{27}Al NMR signal (65% of the original value) with Na(H)- compared to Na(NH_4)-BEA zeolite as shown in Figs. 3 and 5. The difference between the value and Si/Al_{FR} estimated from the NMR spectra and that of chemical analysis represents the concentration of extraframework aluminum. Chemical analysis of H-BEA and Na(H)-BEA zeolites indicated leaching of aluminum from the H-BEA zeolite as a result of Na^+ ion exchange, i.e., the exchange

of a part of extraframework aluminum species, probably Al cations. As follows from d_3-acetonitrile adsorption and Al site quantitative analysis, the presence of extraframework aluminum does not restrict accessibility of the Al-related sites (Table 6). Thus the zeolite channels are accessible for reactants or for metal ions during ion exchange.

Both ^{29}Si bands observed below −102 ppm significantly increase in intensity in the CP experiment and thus they must be attributed to the Si–OH species. The band at −101.1 ppm corresponds to the Si(3Si,1OH) [22,34]. Its intensity significantly increased with zeolite dealumination and can be attributed to Si–OH groups at defect sites after extraction of Al from the framework. The band at −95.5 ppm was formed after framework dealumination and likely corresponds to silanol groups in defect sites.

Corma et al. [34] and Borade et al. [16] found a weak band at −98.0 ppm in beta zeolites, which they attributed to Si(2Si,2Al), i.e., to Al–O–Si–O–Al pairs. This band was not observed in the spectra of Na(NH_4)-BEA and Na(H)-BEA and the observed band at −95.5 ppm cannot be ascribed to such species, because the low energy shoulder in HPDec spectra can be satisfactorily simulated using the corresponding CP spectrum. Moreover, framework aluminum content, estimated for NH_4-BEA from ^{29}Si NMR under the assumption that only Si(3Si,1Al) atoms are present in the framework, corresponds to that one determined from chemical analysis. It implies that the Al–O–Si–O–Al pairs are not present in the framework of both Na(NH_4)-BEA and Na(H)-BEA zeolites. Therefore, only one Al atom can be located in four- and five-membered rings. Thus the cationic sites for the Co(II) ions are represented by six rings, where Al atoms are separated by two Si atoms. This conclusion is in agreement with our suggestion on the Co(II) sites in beta zeolite based on the Co(II) ion Vis spectra, where all three suggested α, β, and γ cationic sites are formed by six rings of the framework of the beta structure [40]. Moreover, this conclusion is in agreement with the Takaishi rule [41] excluding location of two Al atoms in the pentasil ring.

Two bands at −110.0 and −115.0 ppm corresponding to Si(4Si) were also reported by Pérez-Pariente et al. [34] and Kunkeler et al. [42]. The band at −115.0 ppm was attributed to Si atoms in T1 and T2 sites [34]. Two Si(3Si,1Al) peaks at −103.0 and −104.8 ppm have not yet been reported, but the presence of such two species and their different populations can explain a drift of the maximum from −104 to −106 ppm of the band corresponding to Si(3Si,1Al), as reported in Refs. [34,42].

The presence of Al(IV)-A (58.7 ppm) and -B (55.5 ppm) species in beta zeolites and a significantly lower amount of Al(IV)-A with dealuminated Na(H)-BEA (Table 5) is in an excellent agreement with the results of van Bokhoven et al. [13] and Roberge et al. [23] on dealumination of beta zeolites. Attribution of Al(IV)-A resonance to Al siting at the individual T sites is so far not clear. Al(IV)-B resonance was attributed to Al atoms in T1 and T2 sites, which are located in different four rings [13]. This enables us to suggest an Al distribution in the β-type cationic sites, which was considered to be formed by planar six rings of the "beta" cage. Al atoms are assumed to be located in T1 or T2 sites on the opposite side of the six rings. Moreover, because only one Al is located in the four rings, the six rings on the opposite side of the "beta" cage do not create a β-site for a divalent cation. It can be concluded that in H-BEA the Al atoms remain in T1 and T2 sites and are preferentially removed from some of the other (T3–T9) framework sites, not yet specified. As it will be shown later, preservation of these Al atoms is decisive for the high activity of Co-beta zeolites.

4.2. Co ion exchange

A dramatic difference has been found in the replacement of Al-related sites by Co(II) ions in NH_4-BEA and H-BEA zeolites (Fig. 7), i.e., perturbed (via hydrogen bonding, broad band at 3200–3700 cm^{-1}) and unperturbed Si–OH–Al groups (3610 cm^{-1}), Lewis sites originated from "tricoordinated" partly framework Al bearing an OH group (3780 cm^{-1}), and Lewis sites represented by extraframework aluminum, at the increasing degree of Co(II) ion exchange. While with NH_4-BEA the first Co(II) exchanged ions replaced predominantly perturbed Brönsted sites, with H-BEA the consumption of Lewis sites prevailed. However, this difference is only apparent as in both cases the Co(II) ions were first exchanged adjacent to the framework sites containing originally close Al atoms, i.e., perturbed Si–OH–Al groups via hydrogen bonding in NH_4-BEA and "tricoordinated" partly framework Al Lewis sites in H-BEA zeolite. The unperturbed Si–OH–Al, which might originate mostly from single Al atoms, were exchanged by Co(II) ions only with NH_4-BEA, but not with H-BEA.

Assuming Co(II) ion exchange at the cationic site containing two framework Al atoms as "bare" divalent cations ligated only to framework oxygen atoms, and formation of one Al-Lewis acid site by dehydroxylation of two Brönsted acid sites, the concentration of framework aluminum in the zeolite (Al_{IR}) can be calculated according to

$$C(\mathrm{Al_{IR}}) = C(\mathrm{BS}) + 2C(\mathrm{LS}) + 2C(\mathrm{Co_{total}}), \quad (7)$$

where $C(\mathrm{Co_{total}})$ is the concentration of Co ions in the zeolite obtained from chemical analysis and $C(\mathrm{BS})$ and $C(\mathrm{LS})$ are the concentrations of Brönsted and Al-Lewis sites, respectively, determined from FTIR spectra of adsorbed d_3-acetonitrile. The estimated concentrations of framework aluminum in Co zeolites and that obtained from chemical analysis are given in Table 6 and Fig. 17. With CoH-BEA zeolites, an acceptable agreement between Al concentration calculated by using Eq. (7) and that determined by chemical analysis was found in the whole range of Co concentrations. This indicates that the Co(II) ions in CoH-BEA were predominantly exchanged at the cationic sites containing two framework Al atoms. On the other hand, with CoNH_4-BEA the difference between the calculated Al concentration

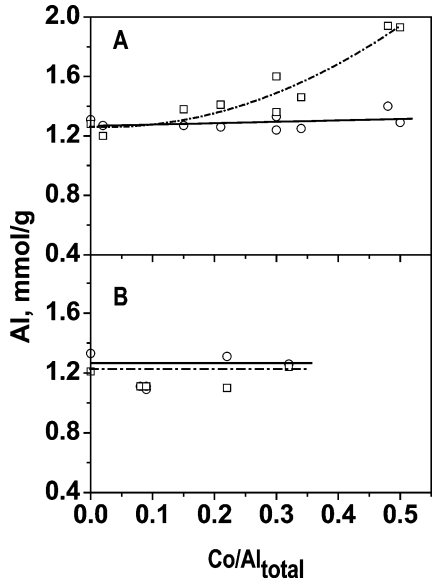

Fig. 17. Dependence of total concentration of Al from chemical analysis (—) and concentration of Al from charge balance, Eq. (7) (–·–), on Co/Al_{total} in (A) $CoNH_4$-BEA and (B) CoH-BEA zeolites.

and that determined by chemical analysis increased with increasing Co ion exchange particularly at $Co/Al_{total} > 0.25$. Therefore, a substantial part of the Co(II) ions at high Co content in $CoNH_4$-BEA can be exchanged as Co-ligand complexes, where one Co(II) ion is balanced by one AlO_2^- framework entity and the extraframework ligand. It should be pointed out an important finding that at $Co/Al_{total} > 0.3$ the increasing amount of Co species present in $CoNH_4$-BEA did not adsorbed d_3-acetonitrile; i.e., these species cannot be ascribed to single "bare"-exchanged Co(II) ions with an open coordination sphere (see Figs. 7A and 17).

4.3. Selective catalytic reduction of NO by propane

Generally, SCR-NO_x with paraffins is a complex process included in the simplest model oxidation of NO to NO_2 and reduction of NO_2 with a hydrocarbon to molecular nitrogen, where activation of a hydrocarbon plays a decisive role. Therefore, various active sites may contribute to the individual steps of the process. While the oxidation of NO to NO_2 has been unambiguously shown to require the redox site, as, e.g., Fe sites in H zeolites [35,36] or Co sites in Co zeolites, reduction of NO_2 can be carried out over protonic or Co sites. It has been also indicated that the distances of the active sites, either H–Co or Co–Co are highly important for the resulting activity [2].

Both $CoNH_4$-BEA and CoH-BEA zeolites exhibited with increasing Co concentration increasing activity in C_3H_8–SCR-NO in the absence of water vapor, reflected in the increased values of maximum conversion of NO to nitrogen and their shift to lower temperatures. It is to be noted that both types of Co zeolites exhibited the same NO_x conversions, if the zeolites contain high and similar concentrations of Co ions in cationic sites (cf. $CoNH_4$-BEA, $Co/Al_{total} = 0.30$, $Co/Al_{FR} = 0.31$, and CoH-BEA, $Co/Al_{total} = 0.32$, $Co/Al_{FR} = 0.48$), as follows from total charge balance, cf. Table 6 and Fig. 17. It implies that the SCR-NO_x activity in the absence of water vapor in the reactant mixture is related to the concentration of Co ions in cationic sites and it is not affected by the conditions of parent zeolite treatment such that the cationic sites containing two Al atoms are preserved.

However, $CoNH_4$-BEA zeolites originated from NH_4-BEA zeolite, where most of the framework Al atoms were Td coordinated in the framework, were much more active than CoH-BEA zeolites in the SCR-NO_x reaction carried out under the presence of water (Fig. 13). In C_3H_8–SCR-NO_x over $CoNH_4$-BEA with $Co/Al_{total} = 0.5$, i.e., with maximum Co ion exchange, the minimum difference between the activity in the absence and presence of water vapor was observed already at 350 °C, when adsorption of water molecules on Co ions is higher compared to a temperature of 450 °C. Moreover, such high activity was stable for ca. 90 h (Fig. 15).

4.4. Active Co sites and Al distribution

High levels of the Co ion exchange in $CoNH_4$-BEA are achieved by the preservation of most of aluminum atoms tetrahedrally coordinated in regular TO_4 frameworks during template removal. Thus regularity of the framework structure and preservation of Al distribution represent a necessary condition for formation of Co ion species exhibiting high activity in the SCR-NO_x under the presence of water vapor. The finding that nearly all the Co ions in CoH-BEA are exchanged in the vicinity of two Al atoms located in one six ring (cationic site), while with $CoNH_4$-BEA in addition a significant part of Co ions is adjacent to a single Al atom in one ring, indicates that the single Al atoms are preferentially removed from the framework during calcinations of zeolite beta under standard conditions. This assumption is supported by a very low concentration of mutually noninteracting Si–OH–Al groups present in the H-BEA zeolite (see Fig. 2).

It can be speculated that removal of the single Al atoms from the framework results in a decrease of the rigidity of the framework and reversible opening of the Si–O–Al bonds in neighboring rings containing two Al atoms and forming the cationic site for a divalent cation. Then the divalent cobalt exchange at this ring, containing two Al atoms, results in removal of this perturbation.

On the other hand, the divalent Co ions adjacent to one framework Al atom should be balanced by an extraframework ligand (e.g., O atom). Therefore, these Co species can be expected not to adsorb weak bases as acetonitrile and water molecules. This is in agreement with the finding that in $CoNH_4$-BEA at $Co/Al_{total} > 0.3$ in contrast to partly dealuminated CoH-BEA zeolites a substantial part of the Co(II) ions do not adsorb d_3-acetonitrile (Fig. 7).

A correlation of TOF values (related to the concentration of these Co species) to cobalt concentration (Co/Al_{total}) in $CoNH_4$-BEA indicates that these Co species might represent the active sites providing high propane–SCR-NO_x activity in the presence of water vapor (see Fig. 16), while the "bare" Co ions at cationic sites exhibit much lower activity.

5. Conclusions

It has been shown that the distribution and state of aluminum atoms in the framework of beta zeolites, controlled by way of template removal from the as-synthesized zeolite, influence dramatically the structure and properties of the exchanged Co species. Calcination of the as-synthesized beta zeolite in an ammonia stream, when the framework negative charge is balanced by NH_4^+ ions, leads to the parent zeolite with highly regular framework and high concentration of both perturbed and unperturbed bridging Si–OH–Al groups (NH_4-BEA). Only a small part of the framework AlO_4 tetrahedra is perturbed by opening of the Al–O bonds with formation of Lewis sites, but with Al still connected to the framework. On the other hand, standard calcination of the beta zeolite in oxygen, yielding protons balancing the framework negative charge, results in an appearance of both perturbed opened framework Al–O bonds and extraframework Al species (H-BEA).

The Co ion exchange occurs predominantly adjacent to two close Al atoms in both $CoNH_4$-BEA (Al Td coordinated) and CoH-BEA zeolites (at Al–O perturbed bonds). Such Co ions exchanged as bare cations at cationic sites containing two Al atoms exhibit high C_3H_8–SCR-NO_x activity, which, however, is substantially decreased in the presence of water vapor. On the contrary, the Co-beta zeolite with high concentrations of regularly Td-coordinated Al atoms in the framework ($CoNH_4$-BEA) contains besides the bare Co ions the Co ion species adjacent to a single framework Al atom, which moreover, do not adsorb base molecules. These Co species are expected to bear extraframework oxygen(s), and they are suggested to be responsible for the high and stable SCR-NO_x activity at high content of water vapor in the reactant stream.

These results imply that the distribution of Al atoms in the framework controls the state and distribution of Co ion species in zeolites, which determine their activity in SCR-NO_x. Preservation of single Al atoms in the framework of beta zeolite after template removal is demanded for formation of Co ions highly active in SCR-NO_x under the presence of water vapor. Template removal from the as-synthesized beta zeolite by its heating in a stream containing ammonia, and thus balancing the framework negative charge by ammonium ions, preserves framework sites from its dealumination.

Acknowledgments

The authors acknowledge financial support from the Ministry of Education, Youth, and Sports of the Czech Republic in the frame of the EC COST 15 Program under Project No. OC- D15.20, and from EU by the Ammonore project #G5RD-CT-2001-00595.

References

[1] X. Wang, H.Y. Chen, W.M.H. Sachtler, Appl. Catal. B 29 (2001) 47.
[2] B. Wichterlová, J. Dědeček, Z. Sobalík, in: G. Centi, B. Wichterlová, A.T. Bell (Eds.), Catalysis by Unique Metal Ion Structures in Solid Matrices. From Science to Application, Prague, 2000, in: NATO Science Series II, vol. 13, Kluwer, Dordrecht, 2001.
[3] Y.J. Li, P.J. Battavio, J.N. Armor, J. Catal. 142 (1993) 561.
[4] G. Bellussi, L.M.F. Sabatino, T. Tabata, M. Kokitsu, O. Okada, EP 652,040 (1994), EniTecnologie S.p.A., Osaka Gas Co. Ltd.
[5] T. Tabata, M. Kokitsu, H. Ohtsuka, O. Okada, L.M.F. Sabatino, G. Bellussi, Catal. Today 27 (1996) 91.
[6] O. Okada, T. Tabata, M. Kokitsu, H. Ohtsuka, L.M.F. Sabatino, G. Bellussi, Appl. Surf. Sci. 121 (1997) 267.
[7] H. Ohtsuka, T. Tabata, O. Okada, L.M.F. Sabatino, G. Bellussi, Catal. Lett. 44 (1997) 265.
[8] H. Ohtsuka, T. Tabata, O. Okada, L.M.F. Sabatino, G. Bellussi, Catal. Today 42 (1998) 45.
[9] B. Wichterlová, Z. Sobalík, J. Dědeček, Appl. Catal. B 41 (2003) 97.
[10] J. Dědeček, D. Kaucký, B. Wichterlová, O. Gonsiorova, Phys. Chem. Chem. Phys. 4 (2002) 5406.
[11] B. Wichterlová, J. Dědeček, Z. Sobalík, in: M.N.J. Treacy, B.K. Marcus, M.E. Bisher, J.B. Higgins (Eds.), Proceeding 12th Int. Zeolite Conf., Baltimore, 1998, Mater. Res. Society, Warendale, 1998, p. 941.
[12] I. Kiricsi, G. Flego, G. Pazzuconi, W.O. Parker, R. Millini, C. Perego, G. Bellussi, J. Phys. Chem. 98 (1994) 4627.
[13] J.A. van Bokhoven, D.C. Koningsberger, P. Kunkeler, H. van Bekkum, A.P.M. Kentgens, J. Am. Chem. Soc. 122 (2000) 12842.
[14] E. Bourgeat-Lami, P. Massiani, F. Di Renzo, P. Espiau, F. Fajula, Appl. Catal. 72 (1991) 139.
[15] L. Beck, J.F. Haw, J. Phys. Chem. 99 (1995) 1076.
[16] R.B. Borade, A. Clearfield, Micropor. Mater. 5 (1996) 289.
[17] L.C. de Menorval, W. Buckerman, F. Figueras, F. Fajula, J. Phys. Chem. 100 (1996) 465.
[18] P.J. Kunkeler, B.J. Zuurdeeg, J.C. van der Waal, J.A. van Bokhoven, D.C. Koningsberger, H. van Bekkum, J. Catal. 180 (1998) 234.
[19] G.H. Kuehl, H.K.C. Timken, Micropor. Mesopor. Mater. 35–36 (2000) 521.
[20] J. Penzien, A. Abraham, J.A. van Bokhoven, A. Jentys, T.E. Müller, C. Sievers, J.A. Lercher, J. Phys. Chem. B 108 (2004) 4116.
[21] E.J. Creyghton, S.D. Ganeshie, R.S. Downing, H. van Bekkum, J. Mol. Catal. A 115 (1997) 457.
[22] A. Fyfe, Y. Feng, H. Grondey, G.T. Kokotailo, H. Hles, Chem. Rev. 91 (1991) 1525.
[23] D.M. Roberge, H. Hausmann, W.F. Hölderich, Phys. Chem. Chem. Phys. 4 (2002) 3128.
[24] L.B. Alemany, Appl. Magn. Reson. 4 (1993) 179.
[25] L. Frydman, J.S. Harwod, J. Am. Chem. Soc. 117 (1995) 5367.
[26] B. Wichterlová, Z. Tvarůžková, Z. Sobalík, P. Sarv, Micropor. Mesopor. Mater. 24 (1998) 223.
[27] S. Kuriyavar, O. Bortnovsky, Z. Tvarůžková, Z. Sobalík, B. Wichterlová, Collect. Czech. Chem. Commun. 66 (2001) 685.
[28] O. Bortnovsky, Z. Melichar, Z. Sobalík, B. Wichterlová, Micropor. Mesopor. Mater. 42 (2001) 97.
[29] Z. Sobalík, Z. Tvarůžková, B. Wichterlová, J. Phys. Chem. B 102 (1998) 1077.

[30] Z. Sobalík, J. Dědeček, B. Wichterlová, D. Kaucký, L. Drozdová, R. Prins, J. Catal. 194 (2000) 330.
[31] M. Maache, A. Janin, J.C. Lavalley, J.F. Joly, E. Benazzi, Zeolites 13 (1993) 419.
[32] C. Pazé, S. Bordiga, C. Lamberti, M. Salvalaggio, A. Zecchina, G. Bellussi, J. Phys. Chem. B 101 (1997) 4740.
[33] O. Bortnovsky, Z. Sobalík, B. Wichterlová, Micropor. Mesopor. Mater. 46 (2001) 265.
[34] J. Pérez-Pariente, J. Sanz, J. Fornés, A. Corma, J. Catal. 124 (1990) 217.
[35] Z. Sobalík, P. Kubánek, O. Bortnovsky, A. Vondrová, Z. Tvarůžková, J.E. Šponer, B. Wichterlová, Stud. Surf. Sci. Catal. 142 (2002) 533.
[36] Z. Sobalík, A. Vondrová, Z. Tvarůžková, B. Wichterlová, Catal. Today 75 (2002) 347.
[37] L. Čapek, P. Kubánek, B. Wichterlová, Z. Sobalík, Collect. Czech. Chem. Commun. 68 (2003) 1805.
[38] P. Sarv, Ch. Fernandez, J.-P. Amoreux, K. Keskinen, J. Phys. Chem. 100 (1996) 19223.
[39] P. Sarv, B. Wichterlová, J. Čejka, J. Phys. Chem. B 102 (1998) 1372.
[40] J. Dědeček, L. Čapek, D. Kaucký, Z. Sobalík, B. Wichterlová, J. Catal. 211 (2002) 198.
[41] T. Takaishi, M. Kato, K. Itabashi, Zeolites 15 (1995) 21.
[42] P.J. Kunkeler, B.J. Zuurdeeg, J.C. van der Waal, J.A. van Bokhoven, D.C. Koningsberger, H. van Bekkum, J. Catal. 180 (1998) 234.